Journal of Stress Analysis
Vol. 4, No. 2, Autumn – Winter 2019-20
Bu-Ali Sina University

Optimization of Effective Parameters on the Nano-scale Cutting Process of Monocrystalline Copper Using Molecular Dynamic

M.M. Abaie[a], M. Zolfaghari[a,*], V. Tahmasbi[b], P. Karimi[a]

[a]Mechanical Engineering Department, Arak University, Arak, Iran.

[b]Mechanical Engineering Department, Arak University of Technology, Arak, Iran.

Article info

Article history:
Received 09 January 2020
Received in revised form
14 March 2020
Accepted 18 March 2020

Keywords:
Nano-machining
Molecular dynamics simulation
Orthogonal nanometric cutting
Response surface method
Optimization

Abstract

Machining in the scale of nanometer and investigating its behavior is premier in the field of machining. Molecular dynamics is a new robust tool to investigate controlling mechanisms in atomic scales, complex dislocation, and grain-boundary in severely deformed workpieces with the submicron dimensioning; consequently, process simulation was performed by molecular dynamics method. In this study, some useful parameters of tool geometry in orthogonal cutting of monocrystalline copper were investigated. With this end in view, relief angle, rake angle, and tooltip radius were considered as influential geometrical parameters of orthogonal cutting of monocrystalline copper. By using the Response Surface Method (RSM), the variation effect of input parameters was studied on the cutting output parameters like cutting force, temperature, and hydrostatic stress all in nanometer precision. Furthermore, with mathematical modeling using a second-order linear regression equation fitted to the process outputs, single objective and multi-objective optimization of the cutting process was followed.

1. Introduction

Ultra high precision machining is a top nanotechnology method for manufacturing nanoscale workpieces and reaching nano surface features [1]. However, considering the limitations of experimentation in the laboratory, machining parameters cannot be directly detected [2, 3]. Molecular dynamics is an alternative to perform such studies. Nano machining of copper is applicable for laser optic and linear acceleration cavity in semi-conducting technology. Moreover, single crystal copper is a perfect substrate for graphene growth has extraordinary electrical properties [4]. There are reports on the effects of parameters on the orthogonal cutting of copper. Nano-machining using a diamond tool is a known process to achieve the desirable surface quality. Komanduri et al. studied the impact of relief angle, rake angle, depth of cut, a width of cut, and tool tip's radius on material behavior for ductile and brittle ones [5, 6]. Promiu stated that cutting force and thrust force and the ratio of cutting force to thrust force all decrease with increasing rake angle. Whereas the ratio of cutting force to thrust force is independent of cutting depth [7] defining the friction coefficient as a function of the ratio of cutting force to thrust force causes a higher friction coefficient for higher rake angles [8, 9]. Pee considered the effect of rake angle on sub-surface deformation and cutting force in the monocrystalline copper cutting process using Morse and EAM potential; it was found that as the rake angle increases, surface quality

*Corresponding author: M. Zolfaghari (Assistant Professor)
E-mail address: m-zolfaghari@araku.ac.ir
http://dx.doi.org/10.22084/jrstan.2020.20790.1124
ISSN: 2588-2597

rises, and cutting force decreases [10]. Ji investigated stress distribution in the tool interface area and cutting force. They studied two different cutting depths, four different cutting speeds, and two rake angles of -30 and -15. They observed as the rake angle became negative, thrust force and friction force increase [11]. Another studies show that For the action of normal force and tangential force, in the grinding process, grinding compressive stress primarily distributes on the front and under the abrasive grain [12, 13]. Wang et al. studied nine different combinations of cutting angles on process output in the silicon cutting process [14]. Dai et al. studied the influence of relief and rake angles and tooltip radius on temperature, force, and subsurface damages. They considered the effect of individual parameters, and their interactions were not studied there [3]. Considering only limited sets of tests causes that one cannot derive a general effect of the rake angle in nanoscale cutting. To better specify the effect of the tool geometry parameters and Their interactional effect, statistical methods, especially the response surface method, are very good [15]. In this paper, the effect of relief angle, rake angle, and tool's tip radius on cutting behavior was investigated. The response surface method was allocated to derive the relation between input and output parameters, clarifying the interactional effects, finding a regression of output parameters, and optimization of the model. With this model, a complete image of the effect of individual parameters as well as interactional effects are obtained as a whole; there is a possibility for optimizing the model.

In this paper, the structure of the workpiece was assumed as a single crystal. Acknowledging severe limitation, it is hardly possible to detect the nanoscale evolution of cutting outputs, e.g., microstructure during machining experimentally. However, it is very desirable to investigate the nanoscale cutting process. Molecular dynamics is an attractive method to study such a process. In this paper, molecular dynamics simulation was used to research nano cutting.

The simulation system consists of two parts, cutting tool and workpiece. A cutting tool was made of carbon, and the workpiece was made of monocrystaline copper. Considering the embedded atom model (EAM) for copper-copper interaction, Tersoff potential for carbon-carbon interactions, and Morse potential for carbon-copper interactions, molecular dynamics simulation was performed.

2. Experiments

2.1. Molecular Dynamics Simulation

This work used Large-scale Atomic/Molecular Massively Parallel Simulator (LAMMPS) to perform all cutting simulation [16]. The simulated outputs were visualized and analyzed by "open visualisation tool" (Ovito) software [17]. Fig. 1 depicts the molecular dynamic system for the single FCC crystalline copper cutting process using Ovito. Simulation parameters are listed in Table 1. Atoms were classified into three divisions, namely boundary atoms, thermostat, and Newtonian atoms. Fig. 1 shows the position of each division. While boundary atoms keep the workpiece fixed and thermostat atoms are used to achieve steady energy and suitable thermal conductivity [18]. In cutting direction, periodic boundary condition and in another direction shrink-wrapping condition were applied to investigate chip behaviour.

Table 1
Input parameters used for molecular dynamics simulation.

Parameter	Value
Workpiece dimension (Å)	$22\times a$, $90\times a$, $17\times a$
Cutting speed (Å/ps)	2.5
Depth of cut (Å)	35
Timestep (ps)	0.0006
Initial temperature (K)	293

By redefining of velocity of thermostat atom, it is possible to keep the temprature of the thermostat atoms close to the desired point, because the thermostat temprature has straight relation with atom velocity.

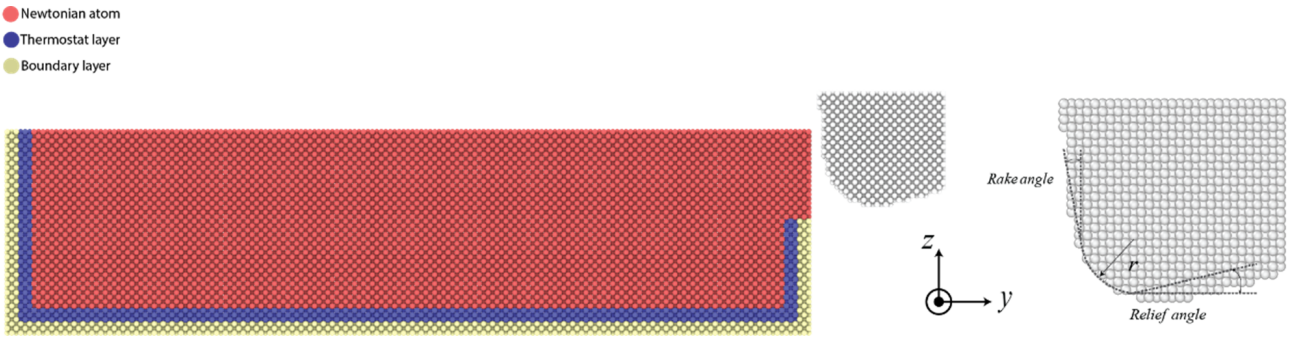

Fig. 1. Illustration of the simulation system.

Though electrons have a negligible effect on thermal conductivity, they can cause a minimal difference between cutting and simulation temperature. The thermostat and Newtonian layers are dynamic, and newton's second law governs their movement. Newton motion equation with a velocity verlet algorithm with 0.0006ps time step was integrated [2]. System size was $22 \times a$, $90 \times a$, $17 \times a$ in Å, where $a = 3.597$Å was the copper lattice parameters. The workpiece size should be large enough to examine the chip behavior. The tool was modeled with a diamond structure. Workpiece coordinate was x-[1 0 0], y-[0 1 0], z[0 0 1] and cutting was performed on (001) surface in [0 -1 0] direction. Three geometrical parameters, namely relief angle, rake angle, and tooltip radius, are illustrated on the tool in Fig. 1. Temperature evolution, cutting forces, and hydrostatic stress were considered as output variables.

2.2. Response Surface Method

In nano cutting process, relief angle, rake angle and tool tip's radius are effective. Investigation of both individual effects of these parameters as well as their interactional effect needs statistical methods whose response surface method is the best [19]. In RSM, the relation between input and output was produced as a linear second-order regression equation. Considering input factor and effective interaction, the general form of equation is presented in Eq. (1) [20].

$$y = \beta_0 + \sum_{i=1}^{k} \beta_i x_i + \sum_{i=1}^{k} \beta_{ii} x_i^2 + \sum_{i} \sum_{j} \beta_{ij} x_i x_j + \varepsilon \quad (1)$$

In Eq. (8) y is the response output based on the input factor, β is the coefficients, x_i is the main input factor of the system, x_i^2 is the square of input factor, and $x_i x_j$ is the second-order interaction of the input factor [21]. The developed model, if accurately derived, can accurately predict the output of the model over the entire range of the input parameters [22].

2.3. Mathematical Modeling and Design of Experiment

In this study considering relief angle, rake angle, and tool's tip radius as input parameters, overall 15 sets of experiments were designed using response surface method and compound center design (ccd).

It should be noted that optimization process was performed on angles that were greater than $-5°$; because in cutting process, the favorite angle was in range $> -5°$. It should be noted that angles lower than $-5°$, reduce surface quality and increase the shear force considerably. Table 2 shows the variation of different input parameters and output variable values in all 15 sets of experiments.

The maximum value of the output parameter during the simulation was selected as the output value Which is used for statistical analysis. Minitab and Design Expert 12 software were used to analyze and interpret the results as well as to obtain the coefficients of the mathematical equation of regression that govern the experiment.

3. Results and Discussion

Shear planes, dislocation, temperature, fault, hydrostatic stress, and force cutting are important factors in nano scale cutting process. However considering the subject of this paper focuses on hydro stress, force, and temperature.

Table 2
Parameters of different sets.

Runs	A°_{relife}	A°_{Rake}	Nose radius (Å)	Temperature (K)	σ_{Hydro}	F_y(eV/Å)	F_z(eV/Å)
1	1	-5	1	381.02	5.71	212.65	181.18
2	15	-5	1	396.76	5.1	188.83	158.58
3	1	15	1	363.62	5.007	220.64	155.57
4	15	15	1	397.35	4.92	143.57	99.53
5	1	-5	20	376.27	6.32	193.30	182.48
6	15	-5	20	380.03	6.32	193.30	169.06
7	1	15	20	383.37	6.28	206.86	183.64
8	15	15	20	380.07	6.26	190.96	163.32
9	1	5	10.5	375.02	5.71	185.82	165.89
10	15	5	10.5	377.76	5.63	177.79	137.70
11	8	-5	10.5	384.07	5.98	164.2	163.91
12	8	15	10.5	378.39	5.36	153.26	121.15
13	8	5	1	390.31	5.38	152.55	123.88
14	8	5	20	382.31	6.19	180.63	153.07
15	8	5	10.5	378.82	5.71	184.44	126.97

Analysis of variance determines the effect of the parameters on the regression equation and plays an important role in analyzing and modeling the experiments [23]. According to the results of analysis of variance and 95% reliability, parameters with P-Value greater than 0.05 were eliminated until no significant decrease in R_{sq} and $R_{sq(adj)}$ was observed.

3.1. The Effect of Input Parameters on Hydrostatic Stress

The modified results from the analysis of variance are listed in Table 3.

Considering the minimum square of error summation for the developed second-order linear model equal to 0.69, the governing equation of the model is according to Eq. (2).

$$\sigma_{Hydro} = 5.316 - 0.01139 \text{ Relief angel} \\ -0.01603 \text{ Rake angle} + 0.05529 \text{ Nose radius} \quad (2)$$

With considering values $R_{sq} = 90.59\%$, $R_{sq(adj)} = 88.03\%$ and $R_{sq(pre)} = 79.54\%$, it can be said that the proposed model possesses an acceptable accuracy.

Increasing the hydrostatic stress in the cutting zone increases the plastic deformation. Hydrostatic stress is an important factor during crack initiation in the cutting zone as can be seen in Fig. 2; the tool tip's radius is the most effective parameter on hydrostatic stress while the effect of the rake angle is low and the effect of relief angle on hydrostatic stress is negligible.

Fig. 3 shows the variation of hydrostatic stress with a simultaneous variation of rake angle and nose radius while keeping the relief angle equal to 8. The reduction of the nose radius and increase in rake angle cause the minimum hydrostatic stress. Moreover, rake angle should be varied more, in comparison with nose radius to initiate similar difference in hydrostatic stress. In the other word, the effect of rake angle is more than that of nose radius. As mentioned before, hydrostatic stress is an important factor during crack initiation in the cutting zone, and classical thermodynamical phase transformation of particles. Fig. 4a shows the change in crystalline structure of workpiece during the cutting for the tool with nose radius of 20Å and rake angle and relief angle of 15 and 1 degree respectively, as can be seen in Fig. 3a, the hydrostatic stress which occurs here is equal to 6.22GPa.

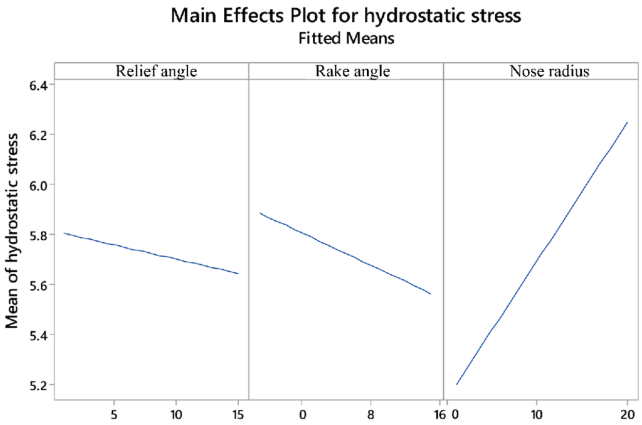

Fig. 2. Main effects plot for hydrostatic stress.

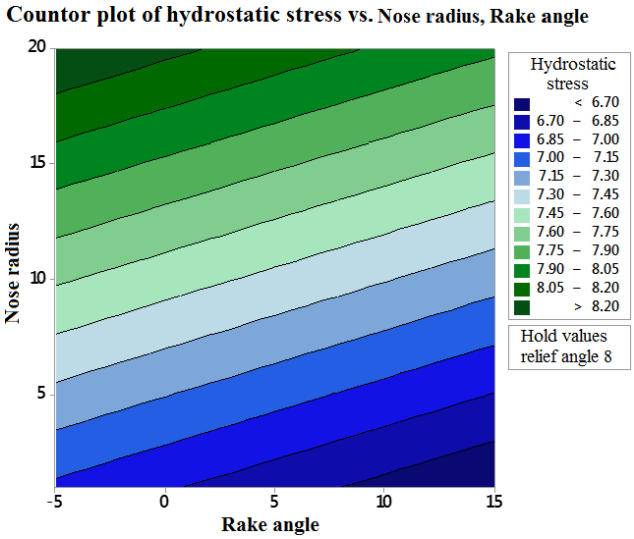

Fig. 3. Contour plot of hydrostatic stress with variation of nose radius and rake angle.

Fig. 4b shows crystalline structure of the workpiece for the tool with nose radius of 1Å and rake and relief angles of 15 degree. As can be seen in Fig. 3, this combination yields to minimum hydrostatic stress equal to 6.4GPa. As can be inferred from Fig. 4, as hydrostatic stress increases, more defects can be detected in the substrate and Surface Roughness increases. Moreover, thermodynamical phase transformation of the particles

Table 3
Analysis of variance of hydrostatic stress.

Source	Contribution	Adj SS	Adj MS	F-Value	P-Value
Model	90.42%	5.2173	1.73910	34.61	0.000
Linear	90.42%	5.2173	1.73910	34.61	0.000
Relief angle	1.84%	0.1061	0.10609	2.11	0.174
Rake angle	7.50%	0.4326	0.43264	8.61	0.014
Nose radius	81.08%	4.6786	4.67856	93.11	0.000
Error	9.58%	0.5528	0.05025		
Total	100.00%				

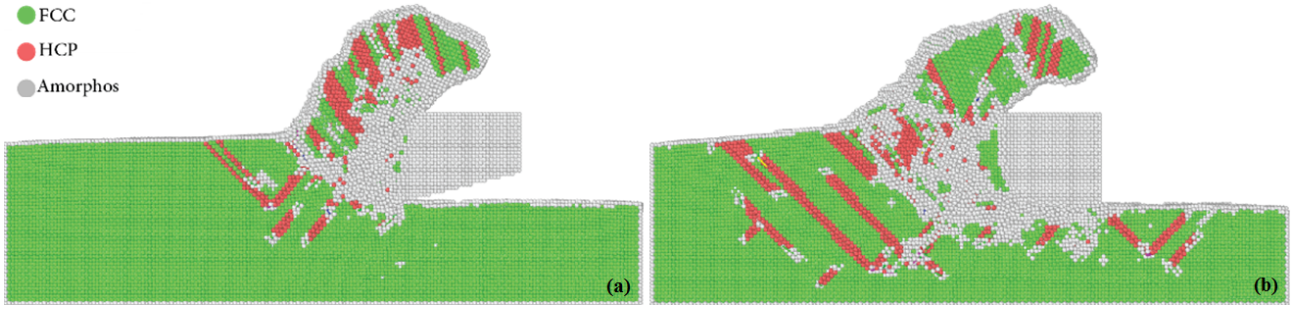

Fig. 4. Deformation and subsurface defects promoted during cutting for a) Experiment set 4, and b) Experiment set 5.

Table 4
Analysis of variance of temperature.

Source	Contribution	Adj SS	Adj MS	F-Value	P-Value
Model	85.58%	852.62	121.80	5.93	0.016
Linear	37.53%	373.93	124.64	6.07	0.023
Relief angle	27.84%	277.41	277.41	13.51	0.008
Rake angle	2.36%	23.56	23.56	1.15	0.320
Nose radius	7.32%	72.95	72.95	3.55	0.101
Square	10.71%	106.74	53.37	2.60	0.143
Relief angle×Relief angle	0.91%	45.14	45.14	2.20	0.182
Nose radius×Nose radius	9.80%	97.63	97.63	4.76	0.066
2-Way interaction	37.33%	371.95	185.97	9.06	0.011
Relief angle×Nose radius	30.14%	300.25	300.25	14.63	0.007
Rake angle×Nose radius	7.20%	71.70	71.70	3.49	0.104
Error	14.42%	143.69	20.53		
Total	100.00%				

is more discernable in Fig. 4a than that in 4b. In Fig. 4a the percentage of the atoms keeping their initial FCC structure is about 66.3% and 8.6% of atoms were transformed to HCP structure. Other atoms about 25.1% lost their crystal structure, meanwhile in Fig. 4b, the percentage of atoms keeping their original structure is about 75.8%.

3.2. The Effect of Input Parameters on Cutting Zone's Temperature

The modified results from the analysis of variance are listed in Table 4.

Temperature distribution's prediction is crucial in obtaining the most possible material removal rate. temperature in the cutting zone depends on the direction and amplitude of the cutting forces and frictional state between tool and workpiece. The heat produced in cutting zone increases the temperature of both tool and workpiece. High tool temperatures can cause softness of the tool and consequently its breakage. The parameters of the regression model derived to predict the temperature are listed in Table 5.

Table 5
Parameters of the regression model derived to predict temperature.

R_{sq}	$R_{sq(adj)}$	Press
85.58%	71.16%	1030.29

Moreover, linear second-order regression equation governing the temperature of the cutting zone is presented in Eqs. (4-10).

$$\begin{aligned} T(K) = {} & 374.04 + 3.031 \text{ Relief angle} - 0.484 \text{ Rake angle} \\ & - 1.079 \text{ Nose radius} - 0.0819 \text{ Relief angle} \\ & - 1.079 \text{ Nose radius} - 0.0819 \text{ Relief angle} \\ & \times \text{ Relief angle} + 0.0654 \text{ Nose radius} \times \text{Nose radius} \\ & - 0.0921 \text{ Relief angle} \times \text{Nose radius} \\ & + 0.0315 \text{ Rake angle} \times \text{Nose radius} \end{aligned} \quad (3)$$

Fig. 5 shows the effect of the relief angle and nose radius while rake angle is kept constant equal to -5, 5, and 15 for Figs. 5a, 5b, and 5c, respectively.

Considering different contours presented in Fig. 5, it can be inferred that increasing rake angle causes a decrease in cutting zone's temperature. It can be attributed to the decrease in friction of the tool tip radius with workpiece and easier flow of the chip. Additionally, the effect of rake angle is lower than other two paprameters, namely nose radius and relief angle. Furthermore, with increase in nose radius, bigger zone of the workpiece comes in contact with tool causing the dissipation of the heat over a larger zone. This easier

heat transfer results in lower cutting zone's temperature.

However, with more increase in nose radius, the worse effect of high process forces is that the produced heat overweighs the positive effect of better heat transfer and increases the temperature of the cutting zone. Decreasing relief angle which causes higher friction and at the same time rises the level of convectional heat transfer mutually leads to a lower temperature of the cutting zone. Because of predominance of heat transfer rate (high) and decrease of nose friction on gathering nose forces (accordingly nose forces increases the nose tempreture), for 15Å raidus and 13° rake angle a minimum temprature is created.

Fig. 6 shows Temperature profile of the workpiece atoms for for a) experiment set 3 , b) experiment set 10, b) experiment set 2, b) experiment set 4

3.3. The Effect of Input Parameters on Process Force

Due to the low numerical dispersion of the forces, the higher capacities of these parameters were used in the analysis of variance and then were obtained by omitting the unsignificant parameters. Regression equations were obtained for anticipating process force which are listed in Table 6.

Table 6
Parameters of regression equation derived for cutting force.

R_{sq}	$R_{sq(adj)}$	$R_{sq(pre)}$
78.93%	63.12%	19.84%
97.42%	92.79%	74.87%

Linear second-order regression equation governing the model to predict the cutting force and thrust force are presented in Eqs. (4) and (5)

$$f_y^3 = 1.02451 \times 10^7 - 1.11497 \times 10^6 \times \text{Relief angle} + 75901.28903 \times \text{Rake angle} - 1.05092 \times 10^5 164 - 12119.96 \times \text{Relief angle} \times \text{Rake angle} + 16497.34955 \times \text{Relief angle} \times \text{Nose radius} + 50727.69287 \times \text{Relief angle}^2 \quad (4)$$

$$f_z^2 = 31737.03706 - 2417.22976 \times \text{Relief angle} - 827.89869 \times \text{Rake angle} - 206.76955 \times \text{Nose radius} - 15.98176 \times \text{Relief angle} \times \text{Rake angle} + 19.18512 \times \text{Rake angle} \times \text{Nose radius} + 29.45053 \times \text{Rake angle} \text{ Nose radius} + 105.71264 \times \text{Relief angle}^2 + 27.11434 \times \text{Rake angle}^2 + 14.71322 \times \text{Nose radius}^2 \quad (5)$$

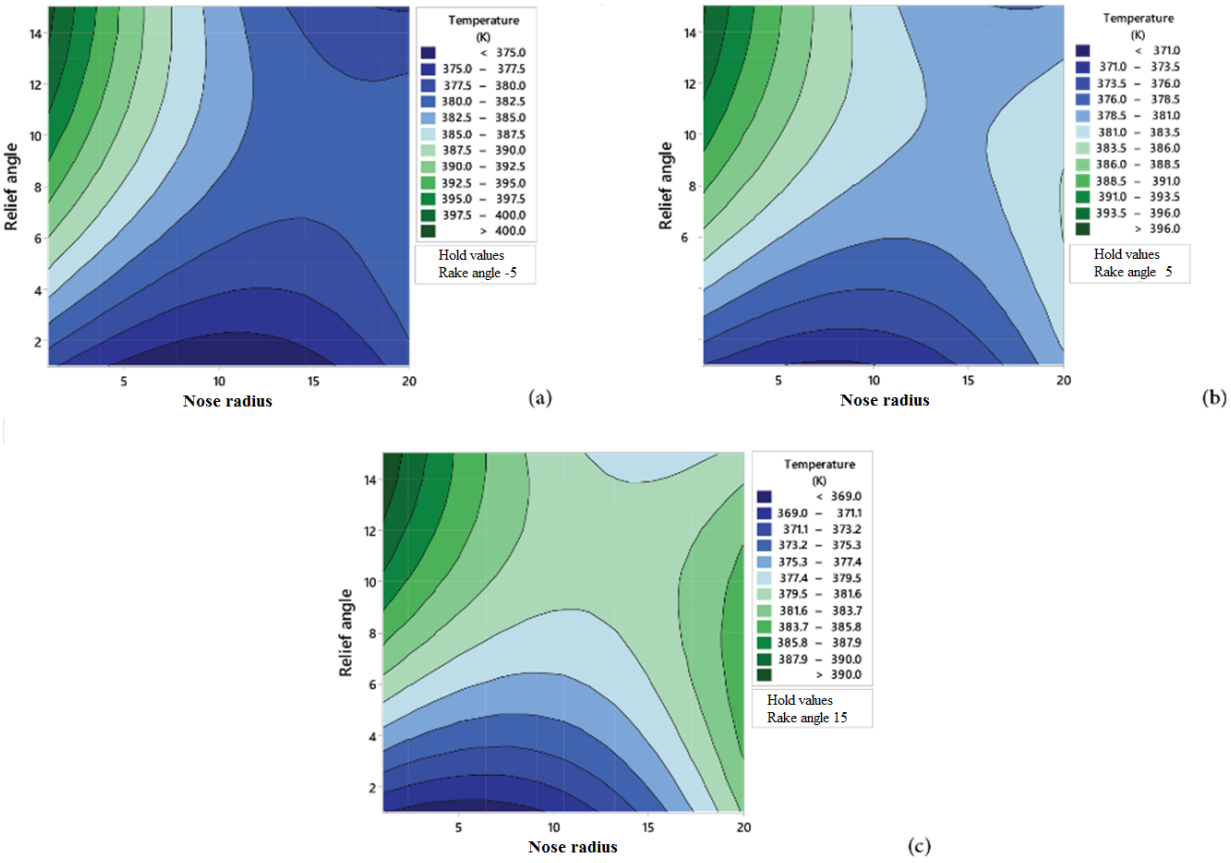

Fig. 5. Temperature variation contour based on nose radius and relief angle for rake angles of a) -5, b) 5, and c) 15.

Cutting forces are very important in cutting process. their increase develops the area of deformed plastic and causes the incidence of an accumulated area of the compact complex structure.

With an increase in relief angle, tool can penetrate the workpiece easier and that causes lower cutting forces. However, excessive increasing in relief angles weakens the tool and so probability of tool breakage. Regarding Fig. 7 showing the variation of thrust force with rake and free angles, when nose radius is kept to 1, 10, and 20Å, the following inferences can be stated.

Firstly, in a negative rake angle and with higher relief angles maximum thrust force occurs and force in this zone is independent of nose radius. Secondly, increasing rake angle causes lower thrust forces which can be explained by the geometry of the chip. However, as nose radius increases, this effect fades away with nose radius of 20Å , at almost all rake angles maximum thrust force occurs. Thirdly, minimum thrust force happens at rake angle higher than 10 and relief angle higher than 11 and nose radius of 5Å.

As the authors know, there is no model for the cutting force, so the model used in this paper is not ideal, considering there is no model better than one presented in this paper as the aouthers know. In other words, to grip a more accurate model to predict the cutting force, more sets of experimentation and higher orders are needed. Nonetheless, an obvious thing from Fig. 8 is that the variation in cutting force is mostly affected by relief angle. Increasing relief angle to its optimum angle around 10° reduces cutting force while more decrease in relief angle causes increase in chips volume, and consequently cutting forces rise. It should be noted that for both thrust and cutting forces, the increase in curvature radius extends the area of cutting forces. Higher cutting forces increase the produced heat boosting up the temperature in cutting zone.

4. Multiobjective Optimization

Relief angle is an effective parameter in the tool-workpiece contact area. Finding an optimum value for relief angle is crucial. If lower than optimum relief angle is selected, higher wear is expected, so contact area between tool and workpiece increases due to severe wear and rising cutting shear forces. Moreover, if higher-than-optimum relief angle is chosen, contact area increases and chips volume boosts up and it leads to increase in cutting forces and produced heat. Rake angle, also, affects genuinely cutting forces, cutting zone temperature, hydrostatic stress, and tool lifetime. According to Fig. 5, with increasing rake angle, cutting zone temperature gradually decreases. This decrease has roots in lower heat production. Finally, increasing rake angle leads to lower cutting forces. Thus, increasing rake angle leads to achieve optimum nanoscale cutting of single crystalline copper. Nose angle is vital in process optimization.

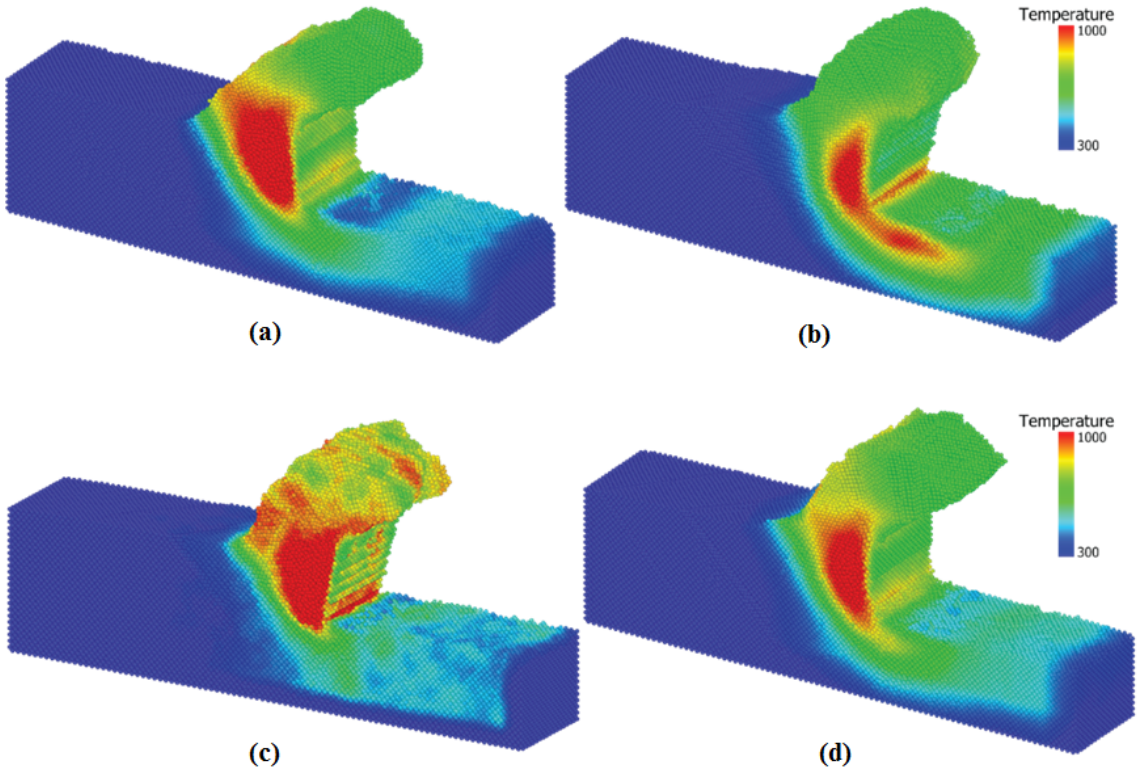

Fig. 6. Temperature profile of the workpiece atoms for a) Experiment set 3 , b) Experiment set 10, b) Experiment set 2, b) Experiment set 4.

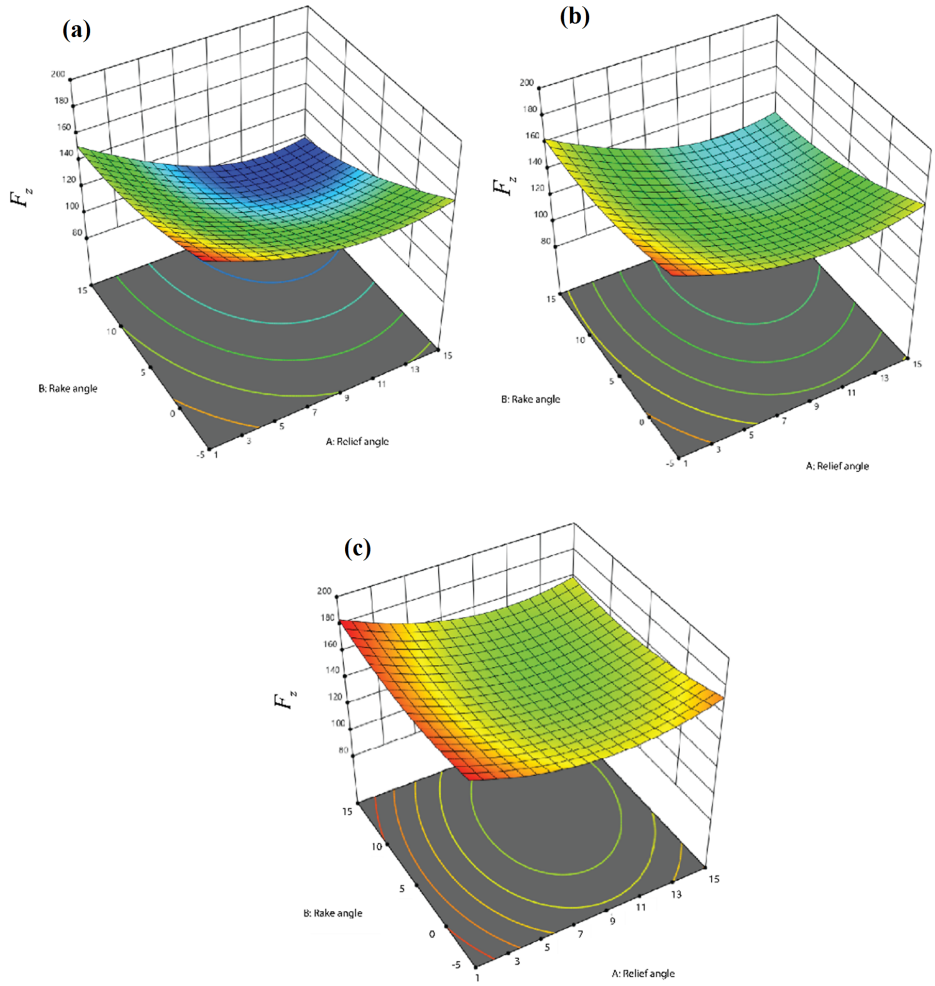

Fig. 7. Countors of thrust force variation with rake and relief angle while keeping nose radius equal to a) 1Å, b) 10Å, and c) 20Å.

Increase in nose radius increases the number of atoms in contact with tool which boost the adhesion force. This can lead to an increase in cutting forces F_y and F_z. Moreover, with increasing nose radius, larger area is in contact and heat is easier dissipated to the bigger area. It eventuates in lower temperatures at cutting zone. However, more increase in nose radius causes higher forces which in turn produce more heat and increase the temperature at cutting zone.

In order to optimize the process, the combination of relief and rake angles and nose radius was obtained by response surface method. Here, two possible scenarios can be thought; first minimization of hydrostatic stress and thrust and cutting forces and second is minimization of cutting zone temperature, Table 7 lists the combination parameters leading to lowest hydrostatic stress and process forces and Table 8 list these parameter for minimum temperature based on response surface models.

Table 7
Optimization of hydrostatic stress, cutting and thrust forces.

Optimization	A°_{relife}	A°_{Rake}	Nose radius (Å)	Temperature	σ_{Hydro}	Cutting force (eV/Å)	Trust force (eV/Å)
RSM modeling	13.23	15	1	389.38	4.98	147.661	96.304
MD simulation	13.23	15	1	396.5	5.01	140.91	87.250
Error%	-	-	-	1.79%	0.59%	4.79%	10.37%

Table 8
Optimization of temperature at cutting zone.

Optimization	A°_{relife}	A°_{Rake}	Nose radius (Å)	Temperature	σ_{Hydro}	Cutting force (eV/Å)	Trust force (eV/Å)
RSM modeling	1	15	1	367.09	5.12	215.79	152.10
MD simulation	1	15	1	363.62	4.97	220.64	155.57
Error%	-	-	-	0. 95%	3.01%	2.19%	2.2%

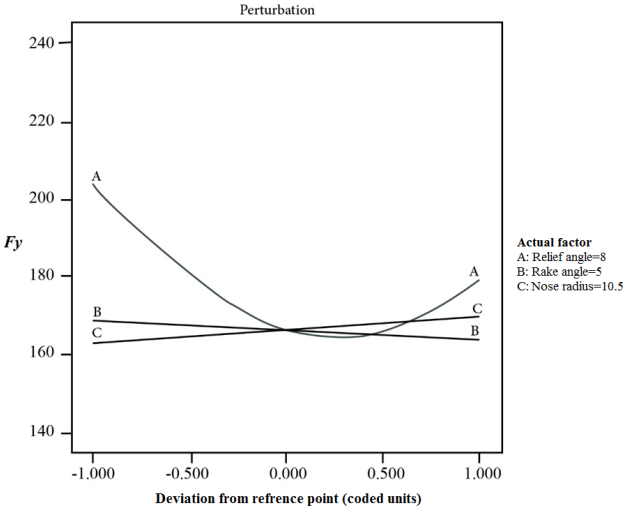

Fig. 8. The effect of each individual parameter on cutting forces when other input parameters are kept constant.

5. Conclusions

In this study, 3D molecular dynamics simulation with response surface method was performed to investigate the effect of important tool geometrical parameters like relief angle, rake angle, and nose radius. The effect of input parameters on hydrostatic stress, temperature, and cutting and thrust forces was studied. The following findings can be highlighted based on the analysis of the RSM model and MD outputs. Hydrostatic stress decreases with nose radius and rake angle. Lower hydrostatic stress leads to lower subsurface defects and better productivity of cutting.

Temperature is minimized with higher rake angles in two distinct areas:

1. Nose radius lower than 10Å and relief angle lower than 5 degree,

2. Nose radius higher than 15Å and relief angle higher than 13 degree.

Minimum thrust force in rake angles higher than 10 and relief angle higher than 11 degree and nose radius of 5Å. The variation in cutting force is mostly affected by relief angle and cutting to optimum relief angle about 10° leads a decrease in cutting force. The minimum hydrostatic stress, cutting force, and thrust force occur in relief angle of 13.23, rake angle of 15, and nose radius of 1Å. The minimum temperature at cutting zone happens with relief angle of 1 degree, rake angle of 15 and nose radius of 1Å.

References

[1] Q. Kang, X. Fang, L. Sun, J. Ding, Z. Jiang, Research on mechanism of nanoscale cutting with arc trajectory for monocrystalline silicon based on molecular dynamics simulation, Comput. Mater. Sci., 170 (2019) 109175.

[2] P.Z. Zhu, Y.Z. Hu, T.B. Ma, H. Wang, Study of AFM-based nanometric cutting process using molecular dynamics, Appl. Surf. Sci., 256(23) (2010) 7160-7165.

[3] H. Dai, H. Du, J. Chen, G. Chen, Investigation of tool geometry in nanoscale cutting single-crystal copper by molecular dynamics simulation, Proceedings of the Institution of Mechanical Engineers, J. Eng. Tribol. Part J, 233(8) (2019) 1208-1220.

[4] A. Sharma, D. Datta, R. Balasubramaniam, Molecular dynamics simulation to investigate the orientation effects on nanoscale cutting of single crystal copper, Comput. Mater. Sci., 153 (2018) 241-250.

[5] R. Komanduri, N. Chandrasekarans, L.M. Raf, Molecular dynamics simulation of the nanometric cutting of silicon, Philos. Mag. B, 81(12) (2001) 1989-2019.

[6] R. Komanduri, N. Chandrasekarans, L.M. Raf, Effect of tool geometry in nanometric cutting: a molecular dynamics simulation approach, Wear, 219(1) (1998) 84-97.

[7] R. Promyoo, H. El-Mounayri, X. Yang, Molecular dynamics simulation of nanometric cutting, Mach. Sci. Technol., 14(4) (2010) 423-439.

[8] Y.Y. Ye, R. Biswas, J.R. Morris, A. Bastawros, A. Chandra, Molecular dynamics simulation of nanoscale machining of copper, Nanotechnology, 14(3) (2003) 390-396.

[9] R. Komanduri, N. Chandrasekaran, M. Raff, M.D. Simulation of nanometric cutting of single crystal aluminum-effect of crystal orientation and direction of cutting, Wear, 242(1-2) (2000) 60-88.

[10] Q.X. Pei,C. Lu, F.Z. Fang, H.Wu, Nanometric cutting of copper: A molecular dynamics study. Comput. Mater. Sci., 37(4) (2006) 434-441.

[11] C. Ji, J. Shi, Z. Liu,Y. Wang, Comparison of tool–chip stress distributions in nano-machining of monocrystalline silicon and copper, Int. J. Mech. Sci., 77 (2013) 30-39.

[12] B. Lin, S.Y. Yu, S.X. Wang, An experimental study on molecular dynamics simulation in nanometer grinding, J. Mater. Process. Technol., 138(1-3) (2003) 484-488.

[13] Z.J. Choong, D. Huo, P. Degenaar, A. O'Neill, Edge chipping minimisation strategy for milling of monocrystalline silicon: A molecular dynamics study, Appl. Surf. Sci., 486 (2019) 166-178.

[14] M.H.Wang, S.Y. You, F.N. Wang, Q. Liu, Effect of dynamic adjustment of diamond tools on nano-cutting behavior of single-crystal silicon, Appl. Phys. A, 125(3) (2019) 176.

[15] R.K. Pandey, S. Panda, Multi-performance optimization of bone drilling using Taguchi method based on membership function, Measurement, 59 (2015) 9-13.

[16] S. Plimpton, Fast Parallel Algorithms for Short-Range Molecular Dynamics, J. Comput. Phys., 117(1) (1995) 1-19.

[17] A. Stukowski, Visualization and analysis of atomistic simulation data with OVITO–the Open Visualization Tool, Modell. Simul. Mater. Sci. Eng., 18(1) (2009) 015012.

[18] Y. Liu, B. Li, L. Kong, A molecular dynamics investigation into nanoscale scratching mechanism of polycrystalline silicon carbide, Comput. Mater. Sci., 148 (2018) 76-86.

[19] V. Tahmasbi, M. Ghoreishi, M. Zolfaghari, Investigation, sensitivity analysis, and multi-objective optimization of effective parameters on temperature and force in robotic drilling cortical bone. Proc. Inst. Mech. Eng. H: J. Eng. Med., 231(11) (2017) 1012-1024.

[20] A. Nekahi, K. Dehghani, Modeling the thermomechanical effects on baking behavior of low carbon steels using response surface methodology, Mater. Des., 31(8) (2010) 3845-3851.

[21] V. Tahmasbi, M. Ghoreishi, M. Zolfaghari, Sensitivity analysis of temperature and force in robotic bone drilling process using Sobol statistical method, Biotechnol. Biotechnol. Equip., 32(1) (2018) 130-141.

[22] V. Tahmasbi, M. Safari, J. Joudaki, Statistical modeling, Sobol sensitivity analysis and optimization of single-tip tool geometrical parameters in the cortical bone machining process. Proc. Inst. Mech. Eng. H: J. Eng. Med., 234(1) (2020) 28-38.

[23] D.C. Montgomery, Design and Analysis of Experiments, John Wiley and Sons Publisher, (2008).